

7. Burke JE, Vadas O, Berndt A, Finegan T, Perisic O, Williams RL. Dynamics of the phosphoinositide 3-kinase p110delta interaction with p85alpha and membranes reveals aspects of regulation distinct from p110alpha. *Structure* 2011; 19:1127-37.
8. Burke JE, Perisic O, Masson GR, Vadas O, Williams RL. Oncogenic mutations mimic and enhance dynamic events in the natural activation of phosphoinositide 3-kinase p110alpha (PIK3CA). *Proc Natl Acad Sci U S A* 2012;109:15259-64.
9. Herman SE, Gordon AL, Wagner AJ, Heerema NA, Zhao W, Flynn JM, et al. Phosphatidylinositol 3-kinase-delta inhibitor CAL-101 shows promising preclinical activity in chronic lymphocytic leukemia by antagonizing intrinsic and extrinsic cellular survival signals. *Blood* 2010;116:2078-88.

Available online April 13, 2017.
<http://dx.doi.org/10.1016/j.jaci.2017.03.026>

Type 3 innate lymphoid cells induce proliferation of CD94⁺ natural killer cells



To the Editor:

Recent discoveries on innate lymphoid cells (ILCs)¹⁻⁶ and innate immune memory⁷ have brought new insights to elucidate the boundary between innate and adaptive immunity. ILCs are a growing family of immune cells, classified into 3 different subtypes (ILC1, ILC2, and ILC3) according to their cytokine and transcription factor expression.^{1,2} They initiate inflammation by promptly producing proinflammatory cytokines in response to multiple stimuli, and can directly influence various immune cells to orchestrate innate and adaptive immune responses.^{1,2} To understand how ILCs might bridge innate and adaptive immunity or further contribute to the expansion of innate immune cells, we asked whether ILCs might affect other immune cells within their surroundings. Using a coculture model, we discovered that ILC3s negative for natural cytotoxicity receptor NKp44 drive a rapid and dramatic expansion of CD94⁺ natural killer (NK) cells. Our data suggest an important link between these 2 cells and a novel function of ILC3s, which may have important basic and translational implications.

ILC1s, ILC2s, and NKp44⁻ ILC3s were isolated from human PBMCs using a protocol previously established in our laboratory. The study was approved by the Swiss Institute of Allergy and Asthma Research Ethics Committee and the Zurich University Human Research Ethics Committee. In brief, we gated on lineage⁻ CD127⁺ viable lymphocytes, of which the CD161^{mid/+} cells were the main ILC population. The 3 ILC subsets were then distinguished on the basis of their differential expression of c-kit, CRTH2, and NKp44 (ie, ILC1: Lin⁻ CD127⁺ CD161⁺ CRTH2⁻ c-kit⁻, ILC2: Lin⁻ CD127⁺ CD161⁺ CRTH2⁺, NKp44⁻ ILC3: Lin⁻ CD127⁺ CD161⁺ CRTH2⁻ c-kit⁺, NKp44⁻) (see Fig E1 and this article's Methods section in the Online Repository at www.jacionline.org). Although ILC3 has 2 distinct subsets, NKp44⁻ and NKp44⁺,⁸ the latter can hardly be detected in peripheral blood in humans, and thus our study using blood samples focused on NKp44⁻ ILC3.

To investigate the interaction of ILC with other immune cells, freshly isolated ILCs were cocultured with carboxyfluorescein succinimidyl ester (CFSE)-labeled autologous PBMCs at an ILC/PBMC ratio of 1:20 in U-bottom plates to enhance cell-to-cell contact (for details, see this article's Methods section in the Online Repository). The cells were cultured for 5 days, a timing

consistent with our experiences with short-term cultures. We first compared the percentage of dividing cells that showed CFSE dilution within total viable lymphocytes in the presence or absence of ILC. As compared with PBMC alone, we found that some cells in the ILC-PBMC cocultures were proliferating (showing CFSE dilution, Fig 1, A). The percentage of dividing cells (R1 in Fig 1, A) within total viable lymphocytes gate were significantly higher in cultures with NKp44⁻ ILC3s compared with control without ILC (Fig 1, B). Cocultures with ILC1 and ILC2 also showed trends of higher proliferation compared with no ILC control (Fig 1, B). The effect of NKp44⁻ ILC3s was particularly notable, where the proportion of dividing cells reached up to 17% to 32%, significantly higher than that of ILC1 and ILC2 (Fig 1, B).

Because the ILCs were CFSE unlabeled and would fall in the "dividing" gate, we next addressed whether the dividing cells have originated from PBMCs or ILCs or both. Phenotyping of the coculture revealed that the cells were mainly CD3⁺ T cells and CD94⁺ NK cells, but not CD14⁺ monocytes or CD19⁺ B cells (Fig 2, A). We also stained for CD4 and CD8 T cells, as well as CD27, CCR7, and CD16 cells. These data demonstrate that ILC3 particularly induced the proliferation of CD94⁺ NK cells and to some degree the CD3⁺CD4⁺ cells, but slight, if any, proliferation of CD8⁺ T cells, and CCR7⁺ and CD27⁺ cells (see Fig E2 in this article's Online Repository at www.jacionline.org). CD14⁺ monocytes cannot be reliably detected after 5-day cultures. Their numbers were too small, which likely represent noise.

The frequencies of various cell types within the total viable lymphocytes are shown in Fig 2, B, revealing that NKp44⁻ ILC3s had the strongest capacity in promoting CD94⁺ cell expansion. The proportion of dividing CD94⁺ cells within total CD94⁺ parental population was also significantly higher than that of CD3⁺ T cells (Fig 2, C), demonstrating the propensity of CD94⁺ cells to proliferate in response to NKp44⁻ ILC3s. The ability of ILC3 in promoting CD94⁺ cell proliferation seemed to occur in the absence of antigen, because our cocultures did not contain antigen-specific stimuli. One of the important findings in this study is that neither of the cells was specifically or nonspecifically stimulated and the culture conditions represent an autologous and spontaneous interaction. It remains an interesting question, if and how antigen and different innate immune response-stimulating substances, such as vaccine adjuvants, might affect this process?

ILCs do not express CD94; thus, the CD94⁺ proliferating cells are NK and to various degree NK-like cells within the PBMCs. CD94 is a transmembrane protein belonging to the C-type lectin superfamily. It forms a heterodimer with NKG2 family molecules to transduce cellular signals. CD94/NKG2 is ligand for HLA-E, a nonclassical MHC glycoproteins class I that is expressed by ILCs (Li S et al, unpublished RNAseq data, 2016). Different to CD16, which is also expressed by macrophage and mast cells, CD94 is mainly expressed on NK cells. Fig E3 in this article's Online Repository at www.jacionline.org depicts CD16 and CD94 expression on freshly isolated PBMCs. In human tonsil, "stage III" immature NK cells defined as CD34⁻ CD94⁻ c-Kit⁺ cells share similar phenotypic markers with ILC3s,⁹ suggesting that these "stage III" immature NK cells might be heterogeneous and potentially composed of ILC3s. It is however unknown whether this knowledge might be applicable to blood ILC3. CD94⁺ cells were the most prominent cell type in response to ILC3-driven expansion, and to a lesser extent CD3⁺ T cells. However, we do

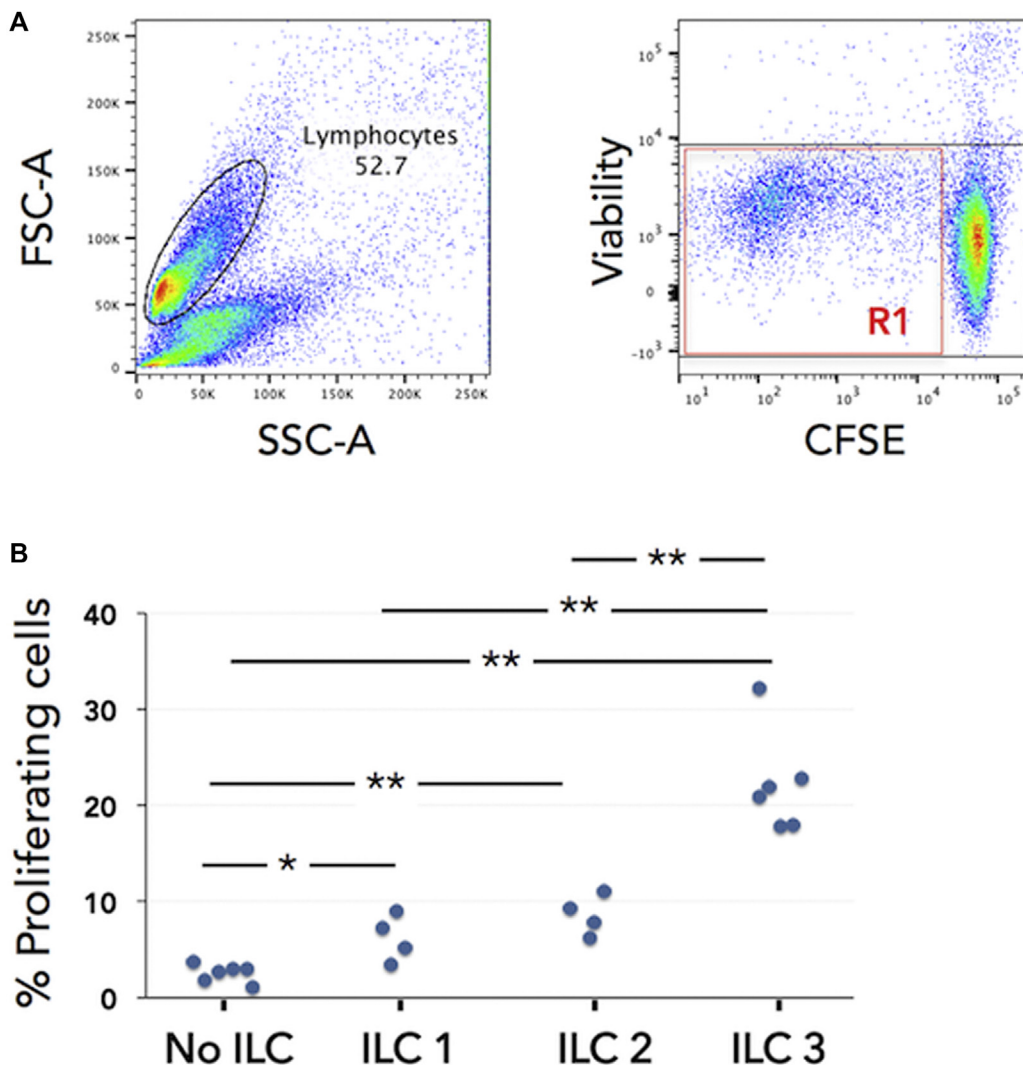


FIG 1. Proliferation of ILC-PBMC^{CFSE} coculture. ILC subsets were cultured with CFSE-labeled autologous PBMCs at a ratio of 1:20. The cultures were harvested on day 5 and analyzed by flow cytometry. **A**, FACS plots depicting proliferation of PBMCs in the presence of ILCs in general. Lymphocytes were gated on the basis of forward and side scatter, and gating out dead cells using a Fixable Viability Dye (eBioscience, Frankfurt, Germany). The region R1 (marked area) depicts the “dividing” (showing CFSE dilution) cells in the presence of ILCs. **B**, Of the total viable lymphocytes, the percentages (% in the y-axis) of “dividing” cells were shown for each coculture. FACS, Fluorescence-activated cell sorting; FSC-A, forward scatter-area; SSC-A, side scatter-area. Data derived from 6 blood samples in 4 independent experiments; ILC3 refers to NKp44⁻ ILC3; Statistics by Mann-Whitney test, **P* < .05 and ***P* < .01.

not know whether ILCs themselves might be proliferating, or other minor cell types such as blood dendritic cells or other cells in the PBMCs might be involved in this apparent ILC3-CD94⁺ cell interaction. We detected a small fraction of proliferating CD94⁺CD3⁺ cells, presumably NK-T cells although their proportions remained minor (data not shown). In some experiments, supernatants of cocultures were collected and analyzed for cytokine expressions. As shown in Fig E4 in this article’s Online Repository at www.jacionline.org, ILC3-PBMC cocultures showed strong trends of increased cytokine secretion compared with ILC1 and ILC2, such as GM-CSF and IFN- γ .

The mechanism of the interaction is unknown. Could cell-to-cell contact be required, and if so, what receptor-ligand pairs are involved? Are soluble factors important, and if so, which soluble factors are necessary and what are their cellular sources?

Additional studies are needed to explore the factors driving NK cell expansion, as well as plasticity between NK cells and ILC3s.

Taken together, our data open a door to important and interesting new studies. Whereas ILC3s are known to promote innate immunity to extracellular bacteria, our findings also suggest that ILC3s may also be involved in innate immunity against tumors and viral infections by rapid expansion of NK or NK-like cells. NK cell memory was reported in recent studies, but mechanisms remain unknown.⁷ Our findings suggest that ILC3 might play a role in NK cell memory development and/or recall. Such a link will provide opportunities for clinical translations, such as in allergy and cancer treatment.

We thank Mark Sleeman from Monash University, Australia, for critical readings.

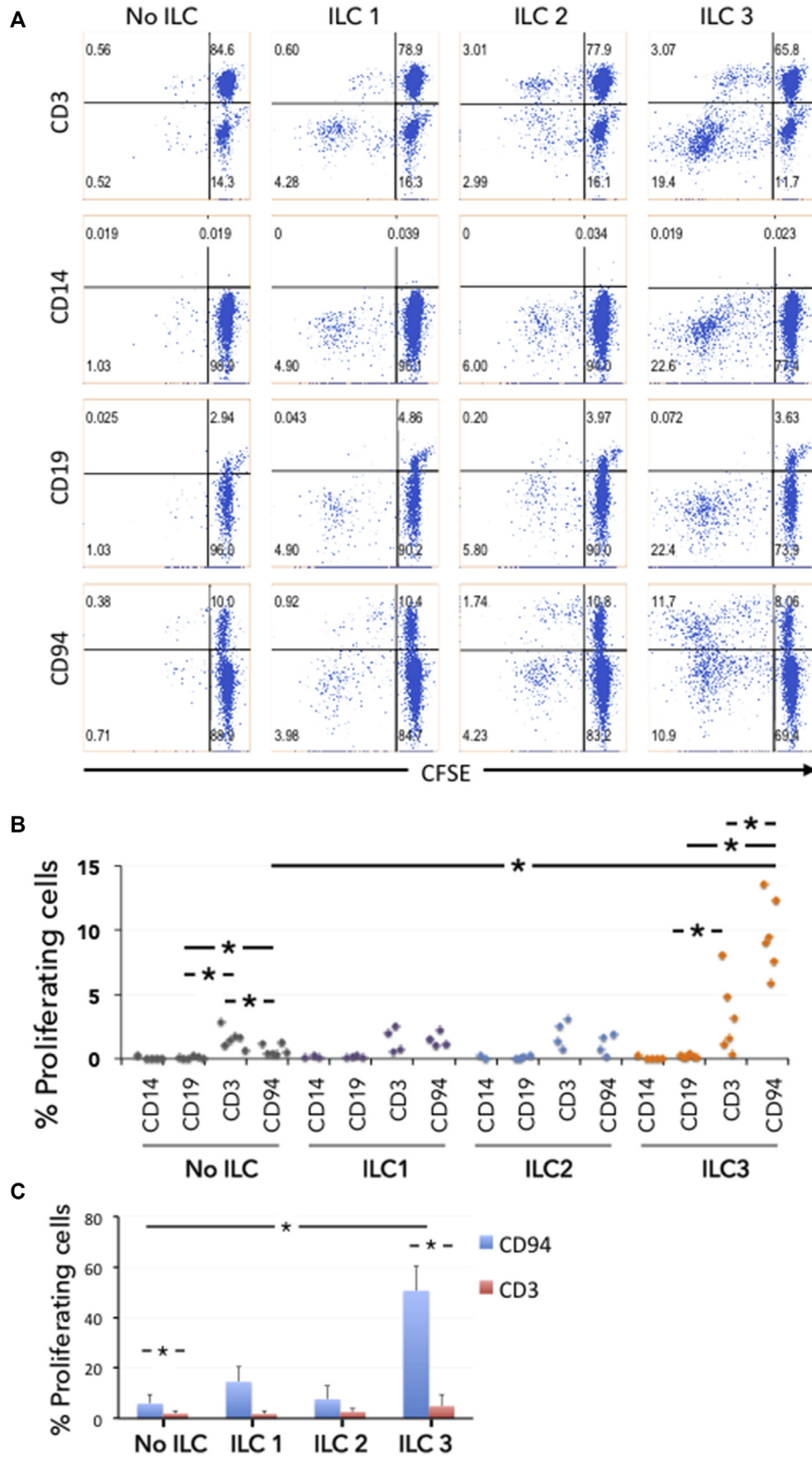


FIG 2. ILC3 drives CD94⁺ cells expansion. **A**, Representative FACS plots depicting “dividing” cell subsets within PBMCs, gating on viable lymphocytes. **B**, Summary of data depicting the proliferation of various cell types in the presence of ILCs. Of each given coculture, the percentages (% in the y-axis) of various cell types within total viable lymphocytes were shown. **C**, Bar plot depicting the extent of CD94⁺ cell and CD3⁺ T-cell expansion in relevance to the parental cell populations, gating on viable lymphocytes: *blue bars* represent the percentage of proliferating CD94⁺ cells within total CD94⁺ cell; *red bars* the percentage of proliferating CD3⁺ cells within total CD3⁺ cell. FACS, Fluorescence-activated cell sorting. Data derived from 6 blood samples in 4 independent experiments; ILC3 refers to NKp44⁻ ILC3; **P* < .05, Wilcoxon matched-pairs signed rank test; Error bar = STDEV.

Shuo Li, PhD^{a,b,*}
Hideaki Morita, MD, PhD^{a,c,*}
Beate Rückert, Sci Tec^{a,c}
Tadech Boonpiyathad, MD^{a,c}
Avidan Neumann, PhD^{a,c,d}
Cezmi A. Akdis, MD^{a,c}

From ^athe Swiss Institute of Allergy and Asthma Research (SIAF), University of Zurich, Davos, Switzerland; ^bthe Department of Microbiology, Monash University, Melbourne, Victoria, Australia; ^cChristine Kühne-Center for Allergy Research and Education, Davos, Switzerland; and ^dthe Institute of Environmental Medicine, UNIKA-T, Helmholtz Center, Munich, Augsburg, Germany. E-mail: akdisac@siaf.uzh.ch. Or: shuo.li@siaf.uzh.ch.

*These authors contributed equally to this work.

This study was supported by the Swiss National Science Foundation (grant no. 310030_156823).

Disclosure of potential conflict of interest: C. A. Akdis serves as a consultant for Actellion, Aventis, Stallergenes, Alergopharms, and Circacia; received grant support from Novartis, PREDICTA: European Commission's Seventh Framework Programme No. 260895 Research on virus-induced exacerbations, Swiss National Science Foundation, MeDALL: European Commission's Seventh Framework Programme No. 261357, Christine Kühne-Center for Allergy Research and Education, and Actellion, Basel. The rest of the authors declare that they have no relevant conflicts of interest.

REFERENCES

1. Mjøsberg J, Spits H. Human innate lymphoid cells. *J Allergy Clin Immunol* 2016;138:1265-76.
2. Morita H, Moro K, Koyasu S. Innate lymphoid cells in allergic and nonallergic inflammation. *J Allergy Clin Immunol* 2016;138:1253-64.
3. Robinette ML, Colonna M. Immune modules shared by innate lymphoid cells and T cells. *J Allergy Clin Immunol* 2016;138:1243-51.
4. Bal SM, Bernink JH, Nagasawa M, Groot J, Shikhagaie MM, Golebski K, et al. IL-1beta, IL-4 and IL-12 control the fate of group 2 innate lymphoid cells in human airway inflammation in the lungs. *Nat Immunol* 2016;17:636-45.
5. Everaere L, Ait-Yahia S, Molendi-Coste O, Vorng H, Quemener S, LeVu P, et al. Innate lymphoid cells contribute to allergic airway disease exacerbation by obesity. *J Allergy Clin Immunol* 2016;138:1309-18.e11.
6. Cols M, Rahman A, Maglione PJ, Garcia-Carmona Y, Simchoni N, Ko HB, et al. Expansion of inflammatory innate lymphoid cells in patients with common variable immune deficiency. *J Allergy Clin Immunol* 2016;137:1206-15, e1-6.
7. Netea MG, Latz E, Mills KH, O'Neill LA. Innate immune memory: a paradigm shift in understanding host defense. *Nat Immunol* 2015;16:675-9.
8. Morita H, Arae K, Unno H, Miyauchi K, Toyama S, Nambu A, et al. An interleukin-33-mast cell-interleukin-2 axis suppresses papain-induced allergic inflammation by promoting regulatory T cell numbers. *Immunity* 2015;43:175-86.
9. Glatzer T, Killig M, Meisig J, Ommert I, Luetke-Eversloh M, Babic M, et al. RORgammat(+) innate lymphoid cells acquire a proinflammatory program upon engagement of the activating receptor Nkp44. *Immunity* 2013;38:1223-35.

Available online April 20, 2017.
<http://dx.doi.org/10.1016/j.jaci.2017.03.033>

Direct monitoring of basophil degranulation by using avidin-based probes



To the Editor:

Basophils are multifunctional effector cells involved in allergic and inflammatory reactions.¹ Basophil degranulation is classically monitored by measuring the amount of mediators (such as histamine) that are released in the extracellular milieu. Alternative methods based on measurement of basophil degranulation using flow cytometry are currently used in clinics.²⁻⁴ Most of those available commercial basophil activation tests rely on the exposure of CD63 or on the upregulation of CD203c on the basophil surface upon allergen challenge.⁵ Yet, these assays do not provide a direct measure of the granule exteriorization process and their results do not always correlate with histamine release.² To take

a step further, we set up a method that allows one to measure the final step of the degranulation process (granule exteriorization) in individual basophils. We have previously shown that fluorescent avidin (that binds the negatively charged proteoglycans composing the granule matrix) can be used to stain exteriorized granules on the degranulated mast cell surface and to quantify degranulation by flow cytometry.^{6,7} Similarly to mast cells, the basophil granule matrix is composed of negatively charged proteoglycans. We thus investigated whether avidin could be used to monitor basophil degranulation.

IgE-sensitized basophils were stimulated with anti-IgE antibodies. Avidin-sulforhodamine (Av.SRho) was added to the incubation medium to monitor degranulation dynamics by time-lapse confocal laser scanning microscopy. Five minutes after stimulation, basophils underwent morphologic changes (eg, increase in cell perimeter and cell spreading) while exteriorized granules were detected on the cell surface (Fig 1, A; see Video E1 and Fig E1, A, in this article's Online Repository at www.jacionline.org). The Av.Srho-integrated fluorescence intensity of the degranulating basophil augmented progressively to reach a plateau 15 minutes after stimulation (Fig E1, B). Taken together, these results show that the addition of Av.SRho to the culture medium allows one to monitor basophil degranulation.

To directly measure basophil-specific activation among white blood cells (WBCs), we analyzed fluorescent avidin binding by flow cytometry. Freshly isolated peripheral WBCs from healthy donors were stimulated with anti-IgE antibodies. Twenty minutes after stimulation, cells were stained with avidin-A488 (Av.A488), anti-CD203c, anti-FcεRI, anti-CD123, and anti-CD63 mAbs and analyzed by flow cytometry. Basophils were identified as CD203c⁺ FcεRI⁺ CD123⁺ cells. Degranulated basophils stained positive for Av.A488 (Fig 1, B). Analysis of the degranulation as assessed by measurement of CD63 exposure or Av.A488 binding provided similar results, by showing that a substantial fraction of the basophil population degranulated for 10 donors in 11 (Fig 1, C and D). In addition, we analyzed in parallel avidin staining, CD63 staining, and histamine released from purified basophils. Scatter plot representations showed a good correlation between the amount of histamine released and the percentage of avidin⁺ or CD63⁺ cells. This analysis shows that fluorescent avidin binding matches the amount of histamine released (Fig 1, E). We next compared Av.A488 staining to CD203c upregulation on basophil surface following stimulation. Basophils from 2 donors in 18 did not respond to anti-IgE stimulation as measured by both methods (see Fig E2 in this article's Online Repository at www.jacionline.org). Noticeably, we observed a discrepancy among the 2 methods in 2 donors (donors 1 and 6) with an increase in avidin staining and no difference in CD203c staining before and after stimulation (Fig E2). To analyze the relative increase in mean fluorescence intensity for the 2 staining procedures, we took advantage of the 2 nonresponder donors (donors 2 and 17) to set the threshold of these tests to relative mean fluorescence intensity (rMFI) = 0.1. This analysis showed that the rMFI calculated using the avidin-based assay did not correlate with the rMFI calculated using the CD203c-based assay. In other words, the 2 methods do not identify the same donors as high responder donors. The discrepancies observed when comparing CD203c- and avidin-based assays could be explained by the fact that avidin staining is strictly associated with degranulation whereas CD203c is a more generic marker of activation. Because priming factors such as IL-3 could impact CD203c upregulation, we investigated whether IL-3

METHODS

Isolation of ILCs

Commercial blood samples from Red Cross were used and the study was approved by Red Cross Oversight Committee. PBMCs were separated using Ficoll-Paque centrifugation. A small proportion of PBMCs were kept aside and labeled with CFSE. The remaining PBMCs were used for ILC isolation. ILC subsets 1, 2, and 3 were isolated from PBMCs as previously described^{E1} with minor modifications. In brief, CD3, CD14, and CD19 cells were magnetic cell sorting (Miltenyi Biotec, Bergisch Gladbach, Germany) depleted and then sorted using a FACS Aria flow cytometer (BD Bioscience, Allschwil, Switzerland). As outlined in Fig E1, lymphocytes were initially gated on the basis of forward and side scatter, and then dead cells were excluded using a Fixable Viability Dye (eBioscience). We then gated on the lineage⁻CD127⁺ viable lymphocytes population, of which the CD161^{mid/+} cells were the main ILC-containing population. The 3 ILC subsets were finally distinguished on the basis of their differential expression of c-kit, CRTH2, and NKp44.

ILC-PBMC coculture

Freshly isolated ILCs as above were mixed with CFSE-labeled autologous PBMCs at a ratio of 1:20, a ratio established on the basis of preliminary experiments. The cells were cultured for 5 days, a timing consistent with our experiences with short-term cultures,^{E2,E3} in complete RPMI 1640 media (supplemented with 10% FCS, 1 mM sodiumpyruvate, 1% MEM nonessential amino acids and vitamins, 2 mM L-glutamine, 100 U/mL penicillin, 100 mg/mL streptomycin) and incubated at 37°C with 5% CO₂. To encourage cell-to-cell contact, we used 96-w U-bottom plate and the cell concentrations were controlled at 1×10^5 cells/200 μ L/well, or as close as possible. The minor cell number variation was caused by insufficient numbers of ILCs in some donors, but the ILC: PBMC ratio was maintained constant.

Flow cytometry analysis

The cocultures were harvested on day 5, supernatants were kept for cytokine analysis, and cells were subjected to flow cytometric analysis. Cells

were stained with Fixable Viability Dye and various surface markers, including CD3, CD94, CD14, CD19, and CD16 (antibodies purchased from BioLegend, München, Germany). An initial lymphocyte gate was set on the basis of forward and side scatter, and additional gates were introduced as required. Flow cytometry was performed using BD Aria III, and data were analyzed using FlowJo online software.

Cytokine measurement in supernatants

Coculture supernatants were analyzed for the presence of cytokines using the Bio-Plex Pro Human Cytokine 27-plex Assay (Bio-RAD, Hercules, Calif) as per manufactures' instruction. In brief, the standard was reconstituted and diluted in a 4-fold dilution series. Culture supernatants 50 μ L were measured without dilution. Luminex (Luminex Corporation, Austin, Tex) was used to read bead fluorescence and results were analyzed using the xPONENT software (Luminex Corporation).

Statistics

We used nonparametric tests to compare the degree of proliferation in various cocultures: Mann-Whitney test to compare total lymphocyte proliferation and Wilcoxon matched-pairs signed rank test to compare between different cell types. The software GraphPad Prism was used for this purpose.

REFERENCES

- E1. Morita H, Arae K, Unno H, Miyauchi K, Toyama S, Nambu A, et al. An interleukin-33-mast cell-interleukin-2 axis suppresses papain-induced allergic inflammation by promoting regulatory T cell numbers. *Immunity* 2015;43:175-86.
- E2. Li S, Jones KL, Woollard DJ, Dromey J, Paukovics G, Plebanski M, et al. Defining target antigens for CD25⁺ FOXP3⁺ + IFN-gamma- regulatory T cells in chronic hepatitis C virus infection. *Immunol Cell Biol* 2007;85:197-204.
- E3. Li S, Floess S, Hamann A, Gaudieri S, Lucas A, Hellard M, et al. Analysis of FOXP3⁺ regulatory T cells that display apparent viral antigen specificity during chronic hepatitis C virus infection. *PLoS Pathog* 2009;5:e1000707.

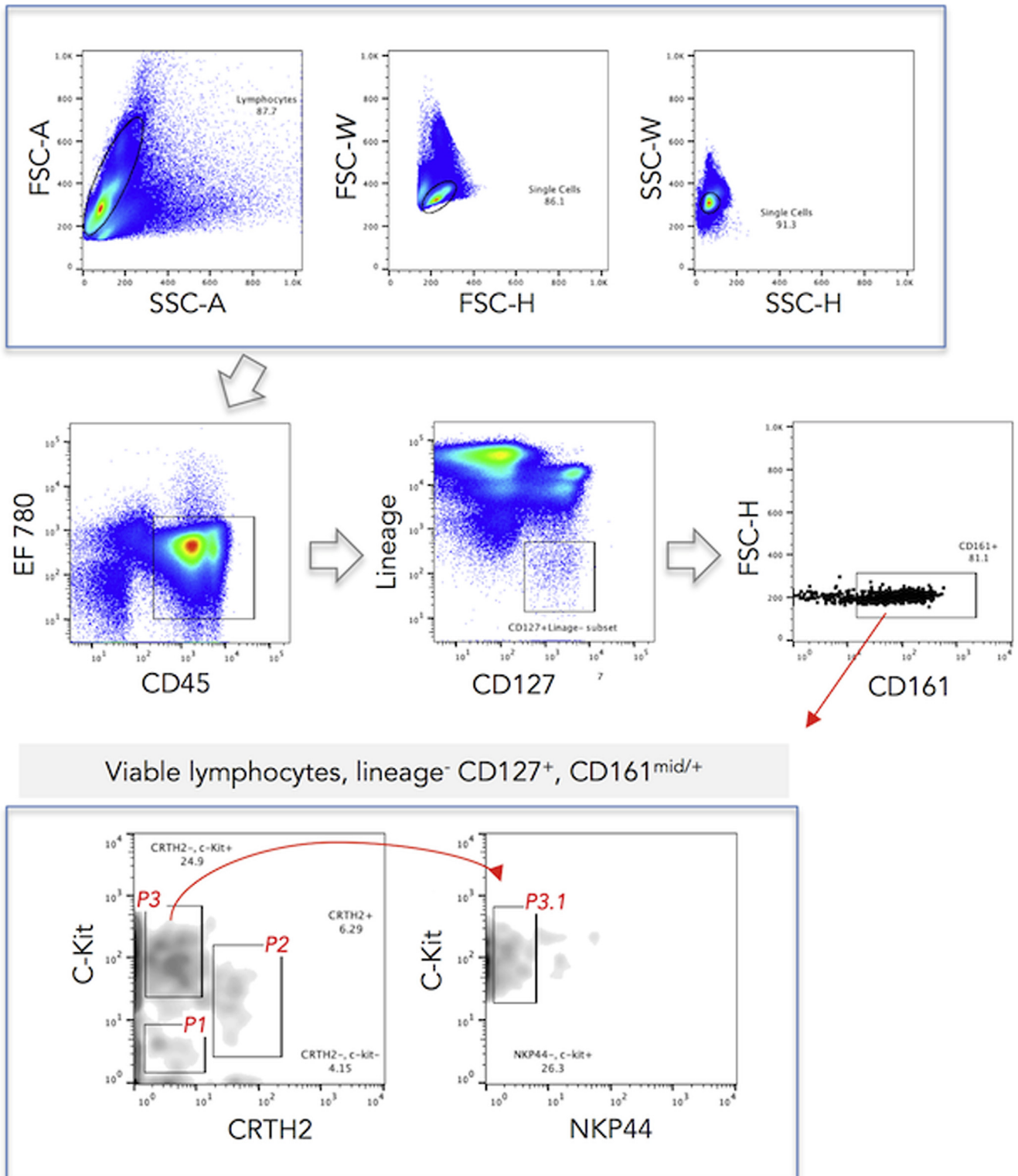


FIG E1. ILC sorting strategy. Lymphocytes were gated on the basis of FSC and SSC, followed by the exclusion of dead cells using Fixable Viability Dye eFluor 780 (eBioscience). We focused on the lineage⁻ CD127⁺ viable lymphocytes population, of which the CD161^{mid/+} cells were the main ILC-containing cell population. The 3 ILC subsets were then distinguished on the basis of their differential expression of c-kit, CRTH2, and NKp44: P1 is ILC1, P2 is ILC2, and P3.1 is NKp44⁻ ILC3. EF780 stands for Fixable Viability Dye eFluor 780. *FSC-A*, Forward scatter-area; *FSC-H*, forward scatter-height; *FSC-W*, forward scatter-width; *SSC-A*, side scatter-area; *SSC-H*, side scatter-height; *SSC-W*, side scatter-width.

A

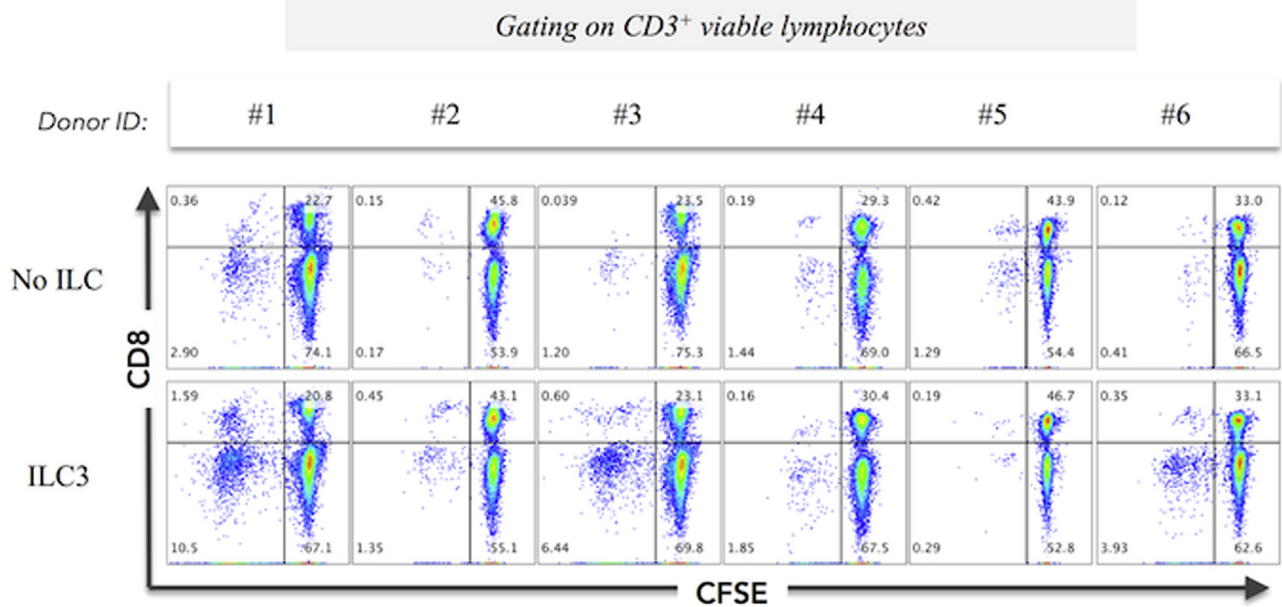
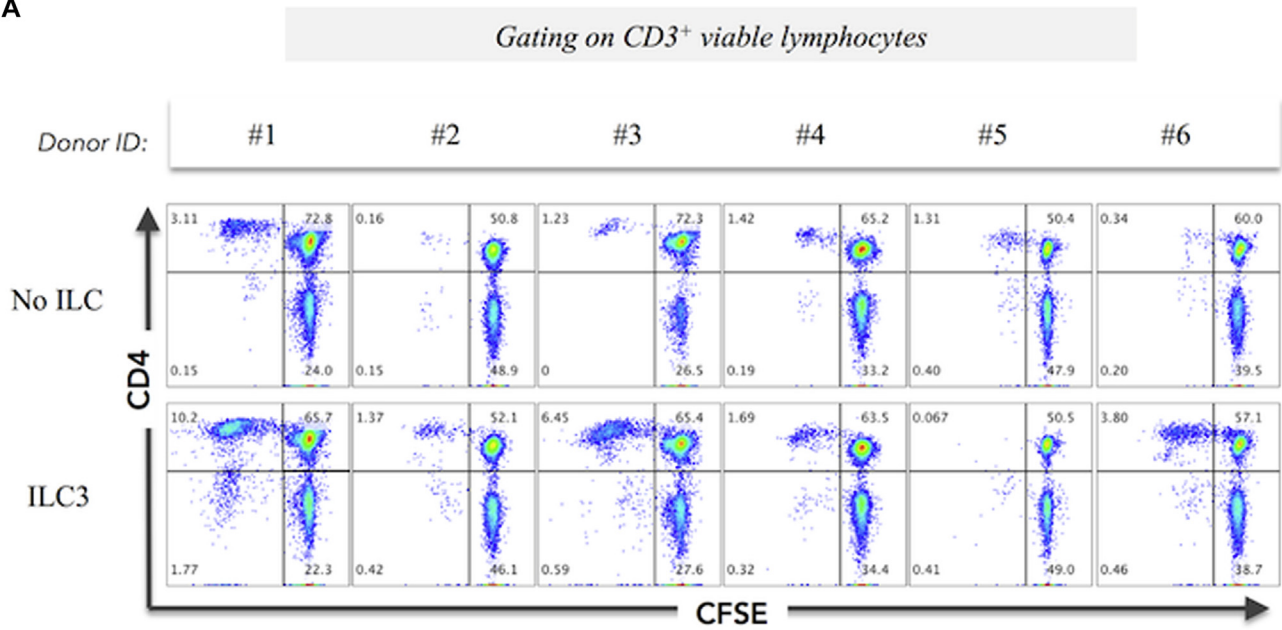


FIG E2. Additional characterization of proliferating cells in ILC-PBMC cocultures. FACS plots depicting proliferation profiles of CD4 and CD8 T cells gated on viable CD3⁺ lymphocytes (A), CD27 and CCR7 expression gated on viable lymphocytes (B), and the expression of CD16 in cocultured cells in relevance to CD94 expression, gated on viable lymphocytes (C). CD16⁺ cells are shown in red dots, and lymphocytes in blue dots. The missing panels indicate when there was not enough ILC to set up the culture. No ILC and coculture with ILC3 was used in all experiments. The data demonstrate that there is some CD4⁺ T-cell proliferation, but slight, if any, additional proliferation in CD8 T cells and CD27 and CCR7 positive cells over cells without ILC conditions. *FACS*, Fluorescence-activated cell sorting.

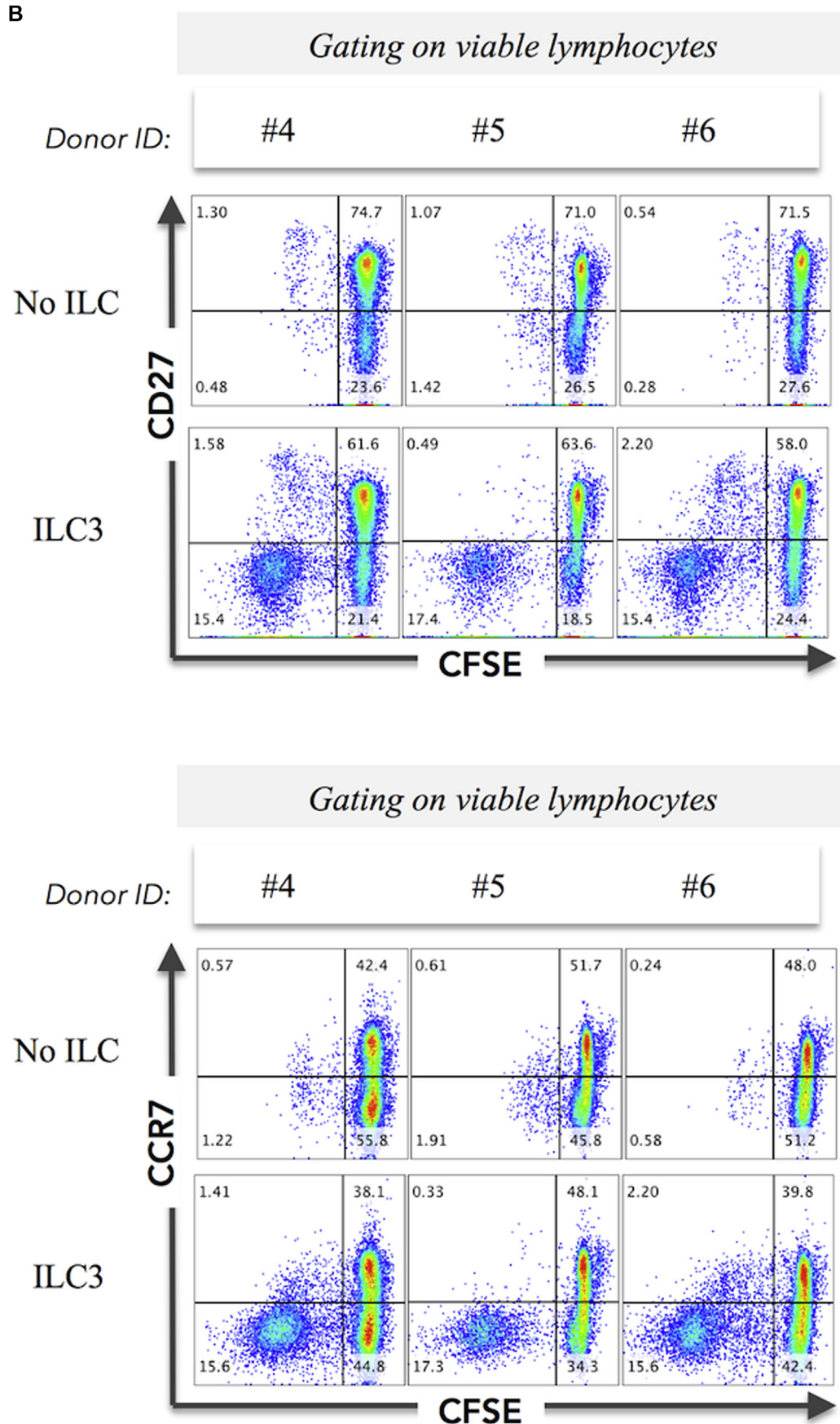
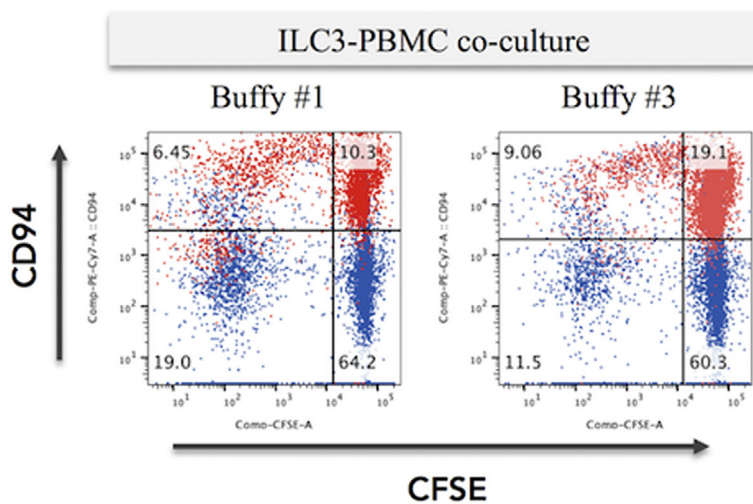


FIG E2. (Continued).

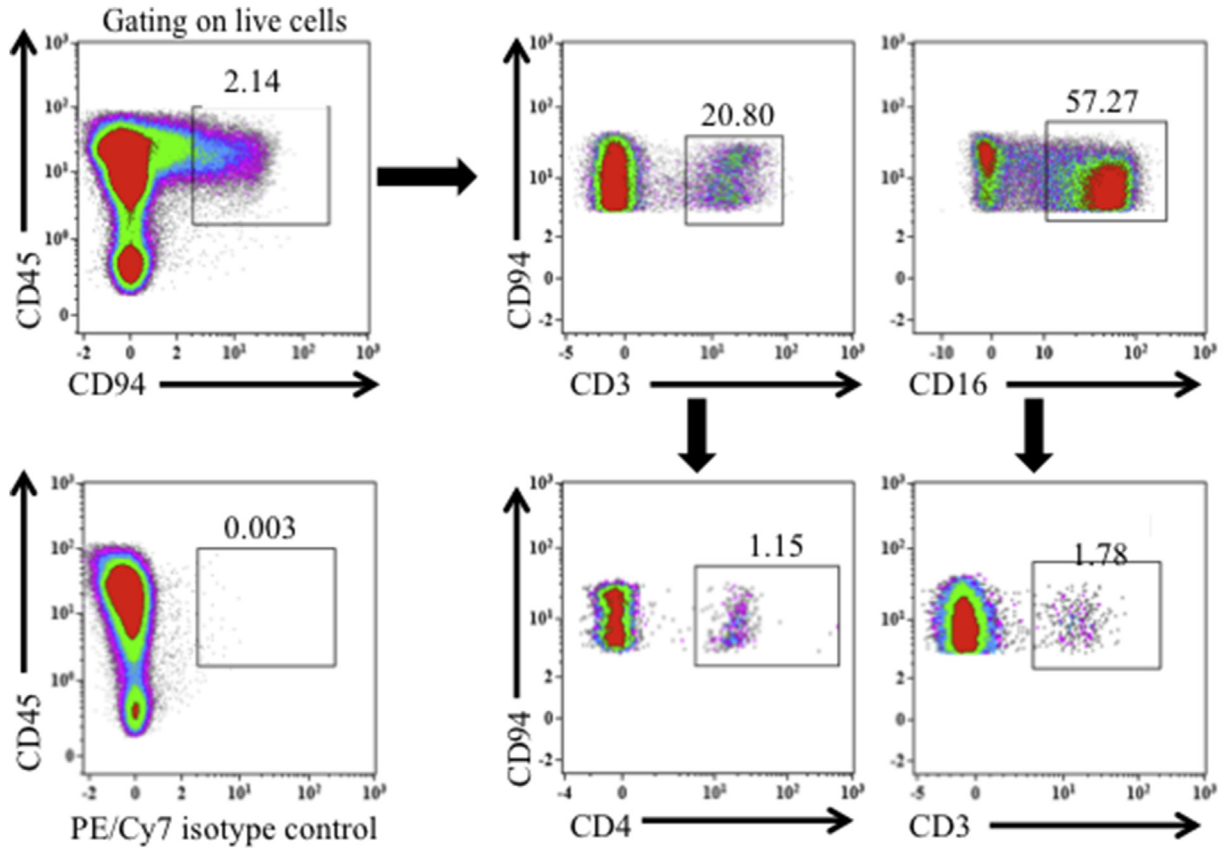
C



% CD16⁺ (in red) within proliferating CD94⁺ cells, in ILC3-PBMC co-cultures

Buffy #1	35.9
Buffy #2	20.2

FIG E2. (Continued).



Percentage and absolute numbers of CD94 expression on CD3⁺, CD4⁺ and CD16⁺ cells

	% CD45 ⁺ CD94 ⁺ (SD)	# cells (SD)/ μ l
CD45 ⁺ CD3 ⁺ CD94 ⁺	20.80 (8.35)	58.34 (32.19)
CD45 ⁺ CD16 ⁺ CD94 ⁺	57.27 (6.04)	160.81 (19.09)
CD45 ⁺ CD3 ⁺ CD4 ⁺ CD94 ⁺	1.15 (1.03)	4.44 (2.60)
CD45 ⁺ CD3 ⁺ CD16 ⁺ CD94 ⁺	1.78 (1.48)	5.61 (3.94)

FIG E3. Quantification of CD94 expression on *ex vivo* CD3⁺, CD4⁺, and CD16⁺ cells. Freshly isolated PBMCs were stained with Viability dye eFlour 780, followed by staining with fluorochrome-conjugated anti-CD3, anti-CD16, anti-CD45, and anti-CD94 mAbs. Cells were gated on live cells (Viability dye eFlour 780⁻) and then gated on CD45⁺CD94⁺ cells. CD45⁺CD3⁺ (T cells) and CD45⁺CD16⁺ (NK cells) were assessed for surface expression of CD94. The dot plot shows the representative gating strategy of CD94 expression on CD3⁺, CD4⁺, and CD16⁺ cell subsets. CD45⁺CD3⁺CD4⁺ (T helper cells) and CD45⁺CD3⁺CD16⁺ (NKT cells) expression on CD94 was gated on CD45⁺CD3⁺CD94⁺ cells and CD45⁺CD16⁺CD94⁺ cells, respectively. The numbers in the plot are averaged and represent the percentage of total CD45⁺CD94⁺ cells belonging to each cell subset. Representative data from N = 3 donors.

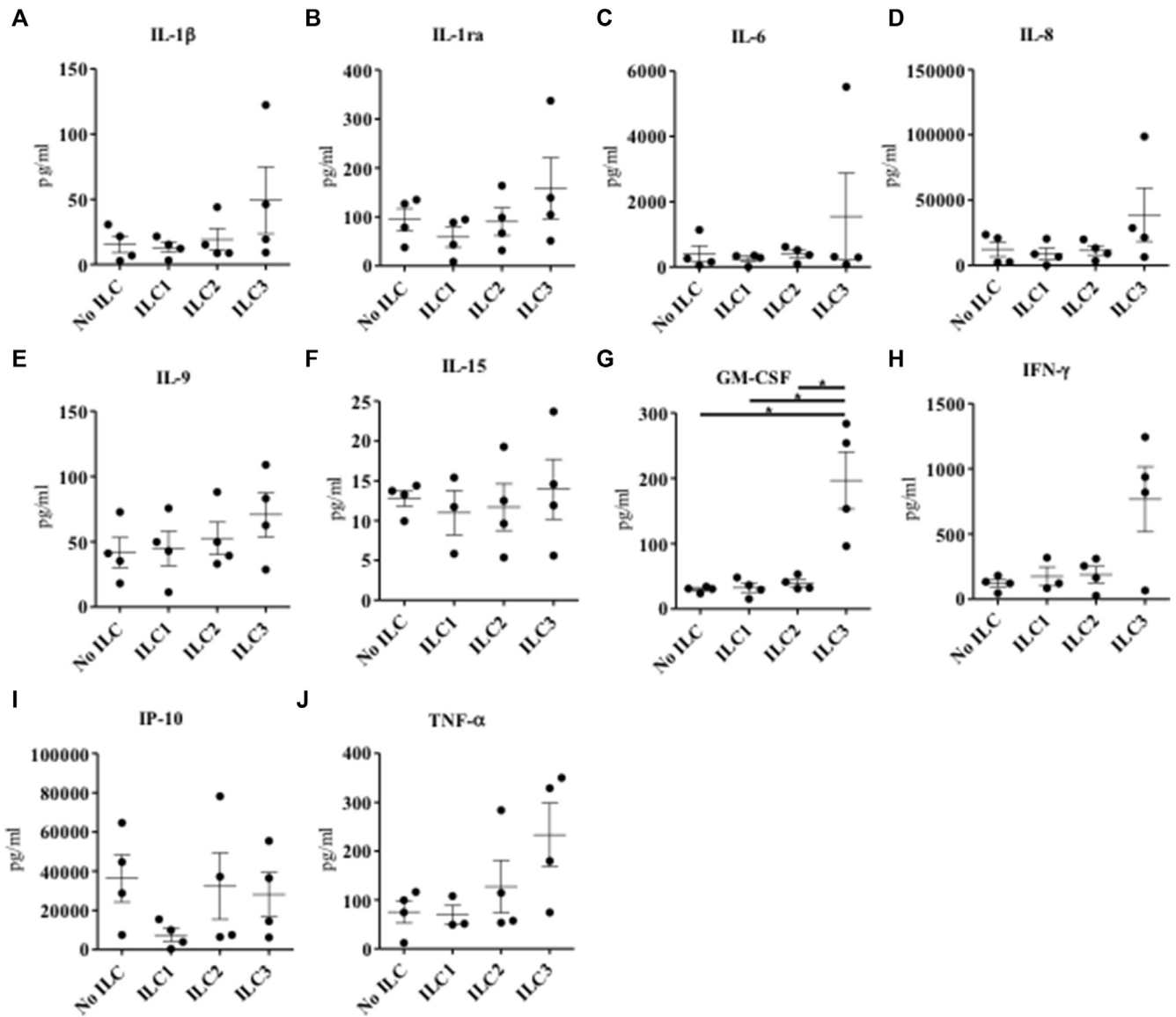


FIG E4. Cytokine levels in supernatants. **A-J,** Cytokine concentrations were measured with a multiplex assay on day 5. *Dots* represent donor's cytokine measurement and the *lines next to the dots* indicate SEM (N = 3). Comparisons between no ILC, ILC1, ILC2, and ILC3 were performed using the Mann-Whitney test. *P < .05.